tvst

Retina

Carboxyamidotriazole Complexed to PLGA Is Safe, Effective, and Durable in Models of Neovascular Retinal Disease

Sergio Li Calzi[1,*], Ayaka Fujihashi[1,*], Dibyendu Chakraborty[1], Yvonne Adu-Rutledge[1], Ram Prasad[1], Edgar L. V. Ready[1], Sarbodeep Paul[1], Srikanth Kakumanu[2], Xiaoping Qi[1], Michael E. Boulton[1], Alan J. Franklin[3], Bob H. Katz[3], and Maria B. Grant[1]

[1] Department of Ophthalmology and Visual Sciences, Heersink School of Medicine, University of Alabama at Birmingham, Birmingham, AL, USA
[2] Department of Clinical Laboratory and Nutritional Sciences, University of Massachusetts, Lowell, MA, USA
[3] ForwardVue Pharma, Mobile, AL, USA

Correspondence: Maria B. Grant, Department of Ophthalmology and Visual Sciences, Heersink School of Medicine, University of Alabama at Birmingham, 1670 University Blvd, Birmingham, AL 35294, USA. e-mail: mariagrant@uabmc.edu

Received: September 30, 2024
Accepted: January 29, 2025
Published: March 25, 2025

Keywords: carboxyamidotriazole (CAI); choroidal neovascularization (CNV); proliferative retinopathy; angiogenesis; age-related macular degeneration (AMD)

Citation: Li Calzi S, Fujihashi A, Chakraborty D, Adu-Rutledge Y, Prasad R, Ready ELV, Paul S, Kakumanu S, Qi X, Boulton ME, Franklin AJ, Katz BH, Grant MB. Carboxyamidotriazole complexed to PLGA is safe, effective, and durable in models of neovascular retinal disease. Transl Vis Sci Technol. 2025;14(3):21, https://doi.org/10.1167/tvst.14.3.21

Purpose: We evaluated the safety and bioactivity of carboxyamidotriazole (CAI) using two approaches, a polymeric CAI-PLGA nanoemulsion in the mouse model of choroidal neovascularization (CNV) and CAI-loaded bioresorbable intravitreal implant in a rabbit model of vascular leakage.

Methods: Mice underwent laser rupture of Bruch's membrane to induce CNV followed by a single (2 µL volume) intravitreal injection of either vehicle ($n = 11$); CAI nanoparticles (0.5 µg, 1 µg, 2 µg, 400 nM, 800 nM, and 1.6 µM, respectively); aflibercept 10 µg; or CAI nanoparticles (1 µg) + aflibercept 10 µg. New Zealand white rabbits underwent either sham intravitreal injection, aflibercept 500 µg injection, or CAI-PLGA intravitreal implant. Vascular leakage was induced with injections of VEGF on days 23 and 53. On days 30 and 60, all groups underwent vitreous fluorophotometry and fundus imaging. On day 60, the rabbits were euthanized, and their eyes were enucleated.

Results: Intravitreal injection of the CAI-Nano at the dose of 1 µg significantly decreased choroidal neovascular volume, to 25% of saline on day 7 and 30% on day 14, which was comparable to aflibercept. Vitreous fluorophotometry revealed significantly lower levels of fluorescein in the aflibercept and CAI implant groups compared to the sham group on day 30. On day 60, the CAI implant group showed significantly reduced neovascularization as compared with the aflibercept groups. No toxicity was observed in any group.

Conclusions: CAI in nanoparticle formulation or as a sustained release bioresorbable implant showed potent efficacy and caused no retinal toxicity in murine and rabbit models.

Translational Significance: CAI demonstrates strong potential as a sustained release anti-angiogenic therapy with effective long-term durability.

Introduction

Neovascular retinopathies, such as age-related macular degeneration (AMD) and diabetic retinopathy (DR), are the two leading causes of blindness in developed countries. Over 2 million Americans are affected by advanced AMD, with an estimated increase to 4 million in 2030. DR affects over 7 million Americans, with a projected increase to 11 million by 2030.[1,2] Moreover, treatment of these diseases is burdensome and costly for both patients and society. For AMD, the total direct healthcare cost in the United States is 575 million dollars, with DR accounting for nearly 500 million dollars.[3] From an economic and work-force standpoint, AMD is projected to cost over

40 billion dollars in productivity loss in the United States.[4] Furthermore, the burden of AMD weighs heavily on patients and society, with an estimated 789,000 years of healthy life lost to this disease.[4] Approximately half of the patients with severe DR have a significantly increased prevalence of vision-related functional burden,[5] and many report a significantly decreased health-related quality of life.[6] The current mainstay of treatment for both AMD and DR involves frequent and on-going intravitreal injections of anti-VEGF agents.

Anti-VEGF therapy represents a quantal advance in our ability to treat these common blinding diseases. However, this treatment paradigm has significant drawbacks, most significantly (1) it is a single biological target in a complex pathophysiological process and (2) durable treatment solutions have been problematic. Even with effective VEGF blockade, only 35% of patients who undergo treatment for neovascular AMD have significant visual improvement and most present with poor vision. Therefore, despite an average of 6 to 8 intravitreal injections per year per treated eye, resultant vision remains poor in about 65% of the patients. Similarly, despite 6 to 8 intravitreal injections per year for people who suffer from diabetic macular edema (DME), 30% are recalcitrant to the standard anti-VEGF injections, which typically manifest as significant vision loss. There are newer generation delivery systems which show some promise and gene therapy trials are underway but there have been notable toxicities and serious adverse events reported. Therefore, there is a large unmet need in the United States and globally for a more effective and durable treatment with a broader mechanism of action for these common blinding diseases.[7,8] A combination anti-VEGF and Ang-2 molecule, faricimab, shows some anatomic benefit to 20% of patients who have persistent exudation during anti-VEGF treatment.[9] Recently, a trivalent Wnt5a-Norrin agonist has shown early results in phase I clinical trials.[10]

Carboxyamidotriazole (CAI), chemically known as 5-amino[4-chlorobenzoyl)-3,5-dichlorobenzyl]-1,2,3-triazole-4-carboxamide is a first-in-class small molecule for ocular disease as a durable anti-angiogenic in an intravitreal product. CAI blocks the Orai1 channel, which is responsible for mediating intracellular calcium concentration. Disruption of Orai1 decreases tube formation and endothelial cell migration; thus, the Orai1 channel is critical in the control of these two pro-angiogenic processes.[11] Orai1 and the VEGFR2 receptor have also been shown to co-localize. In addition to the calcium and VEGF pathways, CAI also inhibits pathological angiogenesis via Wnt-Norrin, fibroblast growth factor (FGF), integrin, and platelet derived growth factor (PDGF) pathways.[12] CAI was also shown to mediate neuroprotective properties by upregulating Bcl-2, decreasing DNA nicking and preserving normal cellular architecture.[13] CAI is a potent inhibitor of posterior segment neovascularization in the mouse oxygen induced retinopathy (OIR) after oral gavage and in laser-induced choroidal neovascularization (CNV) models after intravitreal injection of a beta hydroxypropyl cyclodextrin emulsion.[14] This potent anti-angiogenic molecule has been shown to be safe in validated animal models based on the lack of toxicity observed in clinical observation, ocular examination, IOP measurement, clinical pathology, histopathological, electroretinograms (ERGs), and visual evoked potential (VEP) testing following intravitreal injection of multiple CAI formulations.[14,15] CAI has also been administered systemically in over 900 subjects who suffered from advanced cancers in National Cancer Institute (NCI) trials. Although high serum plasma protein binding and variable oral absorption limited the efficacy of this molecule, the systemic safety profile of CAI showed little toxicity after oral administration.[16–18]

With a significant body of safety and efficacy data in hand, we chose to complex CAI to the well characterized polymer polylactic-co-glycolic acid (PLGA) with the intent to develop safe, durable, and potent anti-angiogenic therapies for common retinal diseases. Polymers of this class have been previously approved for use in ocular indications by the US Food and Drug Administration (FDA) and other regulatory agencies. In this series of studies, we evaluated two different configurations for delivery of bioeffective doses of CAI to the retina; an injectable nanoparticle solution and an injectable bioresorbable implant configuration.

Methods and Materials

CAI-PLGA Nanoparticle Formulation

Solvent Phase

The solvent phase was prepared by adding 200 mg of CAI into a 20 mL scintillation vessel and adding 20 mL of acetonitrile solvent. This produced the solvent phase product, which was then added to varying stabilizer solutions. The process could produce 158 nm particles using a 1:3 ratio solvent to antisolvent composed of 98% BSS, 1% PVA, and 1% Pluronic F68.

CAI-Nano Production

CAI was sourced from the NCI for both studies. The 50 mg of CAI was dissolved in 20 mL acetonitrile.

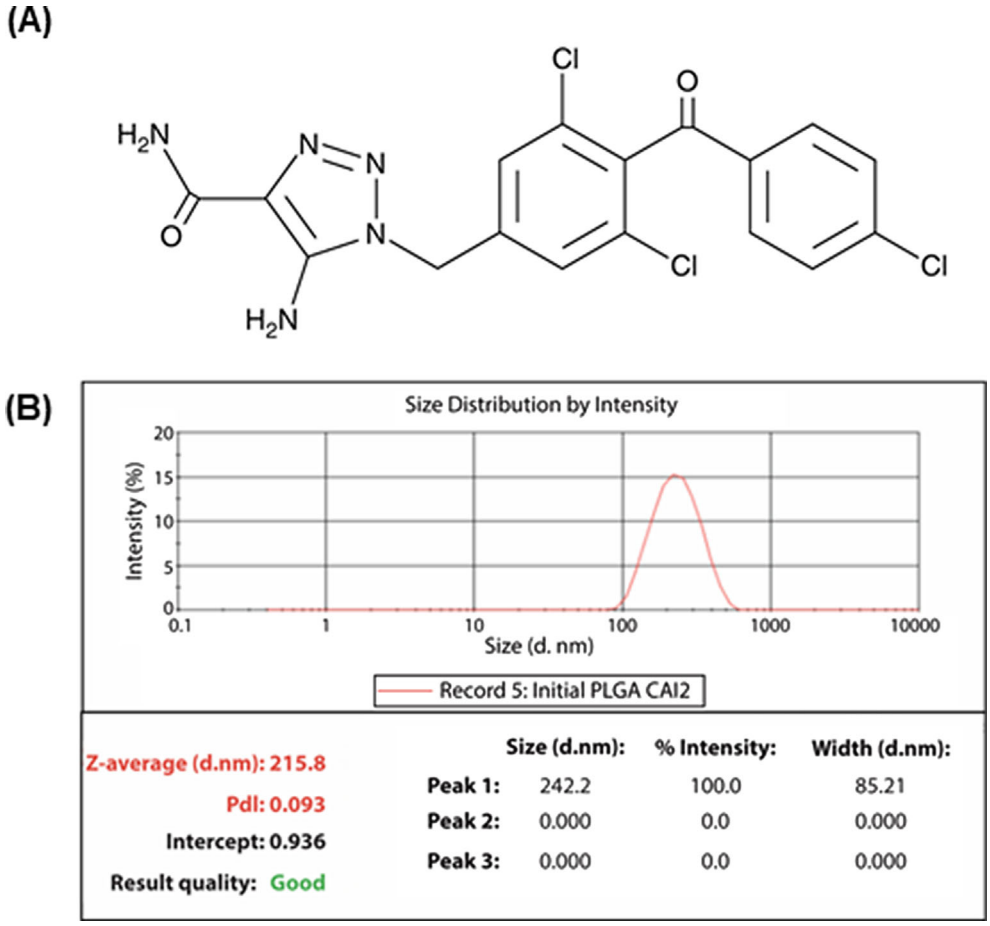

Figure 1. Structure of CAI and CAI nanoprecipitation studies. (**A**) The 5-Amino-[4-(4-chlorobenzoyl)-3,5-dichlorobenzyl]-1,2,3-triazole-4-carboxamide commonly named carboxyamidotriazole (CAI). (**B**) CAI-PLGA nanoparticle incorporation and size distribution. Nanoprecipitation was used for producing polymeric CAI-PLGA nano emulsion that were below 220 nm and with a 0.2 polydispersion index (PDI).

PLGA was purchased from Sigma-Aldrich (product number, 85:15 lactide:glycolide ratio, MW 66-106 kDa). Acetonitrile (99.8%, anhydrous) was purchased from Sigma-Aldrich (271004). The 200 mg of PLGA (66–106 k) was dissolved in 20 mL acetonitrile. BSS buffer (Alcon, Ft. Worth, TX, USA) was used as an antisolvent with 1% Tween-20. One gram of material was added to the BSS buffer and mixed using a magnetic stirrer at 300 rpm for 10 minutes at room temperature. When making the stabilizer/antisolvent, after the stabilizers (Pluronic F68, PVA or HPMC or Tween-80 or Tween 20) were dissolved completely in BSS buffer, the solution was filtered with a 0.22 µm pore size 1L Corning filter with a polyether sulfone (PES) membrane under vacuum. Pluronic F68 (Lutrol) was purchased from BASF (51633115), and Polyvinyl Alcohol (PVA) was purchased from Sigma-Aldrich (P8136, 10-30 kDa).

High-Performance Liquid Chromatography. Analysis Accurately weighed individual samples were placed into 7 mL glass, screw-cap vials. Then, 5.0 mL acetonitrile was added, and the mixture was sonicated for 15 minutes or until fully dissolved. Then, 2.5 mL of the sample solution was placed into a 5 mL volumetric flask and diluted to volume with water. The tubes were prepared for high-performance liquid chromatography (HPLC) analysis by centrifuging an approximately 1.5 mL sample for 5 minutes at 15,000 rpm and immediately transferring a portion of sample off the top to an appropriate HPLC vial with insert. HPLC analysis was performed under the following conditions described in Figure 1B.

CAI-PLGA Bioresorbable Implant

CAI-PLGA Bioresorbable Implant Formulation

Formulation development for the bioresorbable implant began with an assumption of an implant with a rod configuration whose physical envelope dimensions approximate, but do not exceed, the size of an Ozurdex (AbbVie) dexamethasone bioerodible implant, that is,

6.0 mm length × 0.460 mm in diameter. This envelope is currently delivered through a 23-gauge needle.

Given the approximate equivalent molecular weights of CAI and dexamethasone, 424.7 g/mol vs. 392.4 g/mol, respectively, we chose to initially formulate our bioresorbable implant utilizing PLGA polymers that are in the same material class as those used for Ozurdex. We started with polymers specified for 3-month degradation times, chosen to provide early indications for degradation and release kinetics of the system. We also evaluated multiple drug loading scenarios to evaluate the effects of drug load on release kinetics. Constituents were weighed, milled, and mixed prior to processing with a proprietary extrusion process. Extrusion parameters were chosen based on the properties and requirements of the constituent materials.

Analytical assay and in vitro release (IVR) methods were developed based on experience with similar materials. Both methods were based on standard HPLC measurement techniques. Linearity, accuracy, and precision were determined for each method and found to be within acceptable limits for both methods and across the range of formulations to be evaluated. Assay linearity, precision, and accuracy were found to be $R^2 = 1.000$, 0.7% relative standard deviation (RSD), and 99.0% to 100.5%, respectively. For the IVR method, linearity, precision, and accuracy were $R^2 = 1.000$, 1.4% RSD, and 99.7% to 103.5%, respectively, which was deemed acceptable for the early prototype development work. Results of the Content Uniformity assays for multiple formulations demonstrated positive outcomes. For the formulation used in the in vivo studies described herein, average recovery was 94.9% label claim (LC) (5.0% RSD).

Animals and Experimental Designs

All animal procedures used in these studies conformed to the NIH Guide for the Care and Use of Laboratory Animals, the ARVO statement for the Use of Animals in Ophthalmic and Vision Research, and with institutional guidelines and approved by the University of Alabama at Birmingham Animal Care and Use Committee (IACUC 21261).

Murine Choroidal Neovascularization Studies

Mice (C57BL/6J) were obtained from Jackson Laboratory (strain #000664) and underwent laser rupture of Bruch's membrane to induce choroidal neovascularization. In the right eye of each mouse, an Iridex laser (Iridex Corp., Mountain View, CA, USA) with settings of 50 µm spot, 100 ms duration, and 200 mW of power was used to puncture Bruch's membrane in three distinct locations approximately one-disc area from the optic nerve. This fixed distance allows the burns to be both reproducible and isolated from each other. The laser produced a bubble which is indicative of a Bruch's membrane rupture and induces choroidal neovascularization.

One single intravitreal injection (2 µl volume) of (1) vehicle; (2) CAI (0.5 µg); (3) CAI (1 µg); (4) CAI (2 µg); (5) aflibercept 10 µg; or (6) CAI (1 µg) + aflibercept 10 µg was administered immediately after laser induction (Fig. 2A). Optical coherence tomography (OCT) was undertaken using the Bioptigen InVivoVue OCT system. OCT scans were acquired to visualize CNV lesion development in cross-sectional retinal layers. Several horizontal and vertical OCT scans were performed per lesion and used to calculate CNV lesion volume. This three-dimensional quantification of CNV lesion volume was performed using an ellipsoid quantification method, as we have previously described.[19]

Rabbit Model of Proliferative Retinopathy

New Zealand White (NZW) rabbits (strain 052) were obtained from Charles River and were housed in single cages on a 12:12 light: dark cycle with food and water ad libitum. These animals were randomly divided into three groups as follows: group A ($n = 5$) receiving a sham intravitreal injection, group B ($n = 6$) receiving single 1300 µg dose of aflibercept (Eylea; Regeneron, Tarrytown, NY, USA), and group C ($n = 9$) receiving the CAI-PLGA bioresorbable implant (CAI-implant), also via an intravitreal injection. All interventions were performed in random order, but all OD, leaving OS as an internal, contralateral control. All animals were sedated with ketamine (10–20 mg/kg) with the right eye being cleaned with 5% betadine drops before intravitreal injections. The administered aflibercept dose was determined by scaling the standard human dose proportionate to the vitreous volume of the rabbit eye, namely by one third.

On day 0, all groups received their respective treatments of saline intravitreal injection, aflibercept injection (1.3 mg to simulate a 4 mg human dose), or CAI-implant, respectively. On days 23 and 53, all groups received a single 10 µg VEGF injection to induce retinal vascular leakage.[20,21] All intravitreal injections were given 3 mm posterior to the corneal limbus after administration of a drop of 10% povidone iodine on the ocular surface. Erythromycin antibiotic ointment was applied to the treated eye following each intervention.

Ocular measurements of vitreous fluorophotometry (VFP), intraocular pressure (IOP), and fundus photography were performed on all groups on days 30 and 60. On day 60, all the rabbits in groups A and

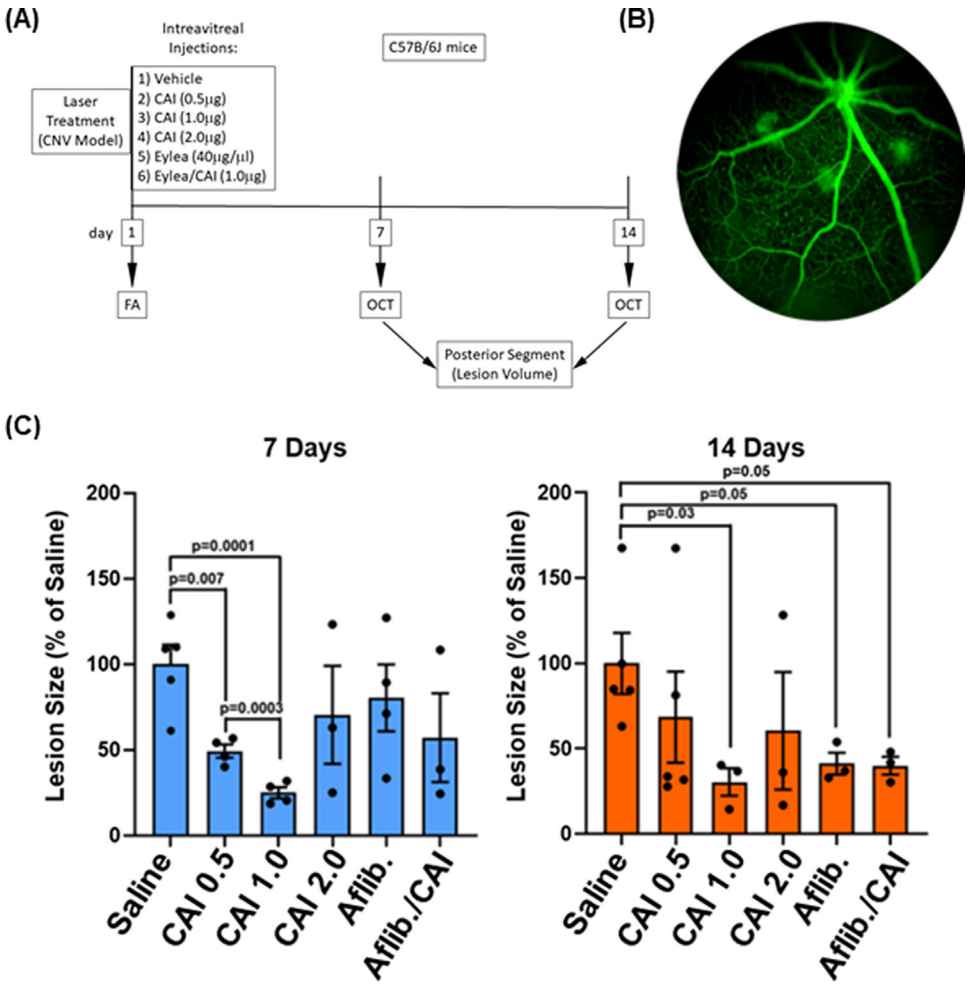

Figure 2. **Study design and assessment of CNV lesions in laser-induced model.** (**A**) Laser induced CNV was used to assess the anti-angiogenic effects CAI-PLGA nano emulsion. Mice underwent laser rupture of Bruch's membrane and subsequently developed neovascularization. One single intravitreal injection of test agent was administered immediately after the laser. (**B**) Laser injury was confirmed by fluorescein angiography (FA). (**C**) One- (*left panels*) and 2-weeks (*right panels*) post laser injury and treatment in each retina was imaged by OCT and laser injury volume was quantified. Quantification of CNV lesions. Intravitreal administration of polymeric CAI-PLGA nanoemulsion, CAI-PN, led to a reduction of CNV volume compared to saline treated eyes based on OCT analysis at 1- and 2-weeks post injection. This angiogenic inhibition compared favorably to aflibercept (Eylea) injections. Combination of the two treatments did not result in an addictive effect.

B, as well as 6 animals from group C, were euthanized post-measurements and their eyes were enucleated. VFP was performed using a Fluorotron Master fluorophotometer (Ocumetrics, Mountain View, CA, USA). The animals were injected with fluorescein through the ear vein and fluorescein was allowed to circulate and diffuse into the eye prior to the photometry measurement 1 hour later.[22] Fundus imaging was performed using a Zeiss Visuoscout 100. IOP measurements were obtained using an AVIA Tono-Pen applanation tonometer (Reichert, Depew, NY, USA).

After enucleation, the eyes were fixed in 4% paraformaldehyde overnight. The eyes were sectioned and stained with hematoxylin and eosin (H&E) and viewed by light microscopy. Images of the retinal sections were captured with Zeiss Axio Q6 Imager Z2 epifluorescence microscope (Zeiss AG, Oberkochen, Germany) and saved as jpeg images. Retinal thickness measurements were performed. Individuals were masked to the treatment cohort of each animal during data collection. Statistical analyses were performed using GraphPad Prism version 9.1 software. Data are reported as mean ± SD. All data were assessed for adherence to normal distribution by the Shapiro-Wilks normality test. Data which conformed to normal distribution were analyzed by the unpaired Student's *t*-test and data which failed to meet the assumptions of normality were analyzed using the unpaired Mann-

Whitney test. The P values less than 0.05 were considered statistically significant.

Results

Injection of Polymeric CAI-PLGA Nanoemulsion Results in Reduced CNV Laser Lesion Size

Nanoprecipitation was used for producing CAI-PLGA nanoparticles that were below 220 nm and 0.2 polydispersion index (PDI) representing a reproducible method to generate nanoparticles of acceptable size and particle size distribution (Figs. 1A, 1B). Wild type mice underwent laser injury and immediately post laser were injected with polymeric CAI-PLGA nanoemulsion (0.5 µg, 1.0 µg, or 2 µg) or aflibercept (10 µg) or the combination of aflibercept and CAI 1 µg in a 2 µL total volume (Fig. 2A). Fluorescein angiography (FA) was used to confirm the success of laser rupture and location of the lesions (Fig. 2B). The volume of the laser burn was quantified using OCT (Fig. 2C, Fig. 3). Seven days post intravitreal injection of the polymeric CAI-PLGA nanoemulsion, a significant decrease in choroidal neovascular volume was observed with a dose-dependent effect for CAI at 0.5 and 1.0 µg doses when compared to saline injected mice (saline = 100 ± 8.93, $n = 5$ vs. CAI 0.5 µg = 49.27 ± 2.89, $n = 4$, $P = 0.0066$, saline versus CAI 1.0 µg = 24.87 ± 2.49, $n = 5$, $P = 0.0001$). However, a higher dose of CAI did not show any significant effect (saline versus CAI 2.0 µg = 70.43 ± 9.08, $n = 3$, $P = 0.295$). Aflibercept (saline versus aflibercept = 80.29 ± 7.93, $n = 4$, $P = 0.388$) or the combination (saline versus aflibercept/CAI 1.0 µg = 57.09 ± 5.08, $n = 3$, $P = 0.127$) did not show efficacy at day 7 suggesting no additive or synergistic effects. On day 14 post treatment, CAI at the 1.0 µg dose showed reduced neovascularization compared to saline (saline = 100 ± 16.72, $n = 5$ versus CAI = 30.52 ± 7.01, $n = 3$, $P = 0.030$). This response compared favorably with the effect of 10 µg intravitreal aflibercept at week 2 (saline versus aflibercept = 41.29 ± 6.95, $n = 3$, $P = 0.052$; see Fig. 2C). There did not appear to be a greater anti-angiogenic effect with increased amounts of CAI-nanoparticles (see Fig. 2C). Combination treatment with 1.0 µg CAI-nanoparticle and 10 µg aflibercept was no more effective than polymeric CAI-PLGA nanoemulsion alone at week 2 (CAI 1.0 µg = 30.52 ± 7.01, $n = 3$, versus CAI/aflibercept = 40.06 ± 2.86, $n = 3$, $P = 0.356$; see Fig. 2C).

Thus, CAI-nanoparticle was more effective at decreasing CNV volume at week 1 compared to aflibercept and was similar to the anti-angiogenic effect from aflibercept at week 2. The CAI-nanoparticle did not show any evidence of toxicity and effectively inhibited neovascularization in the laser-induced CNV model.

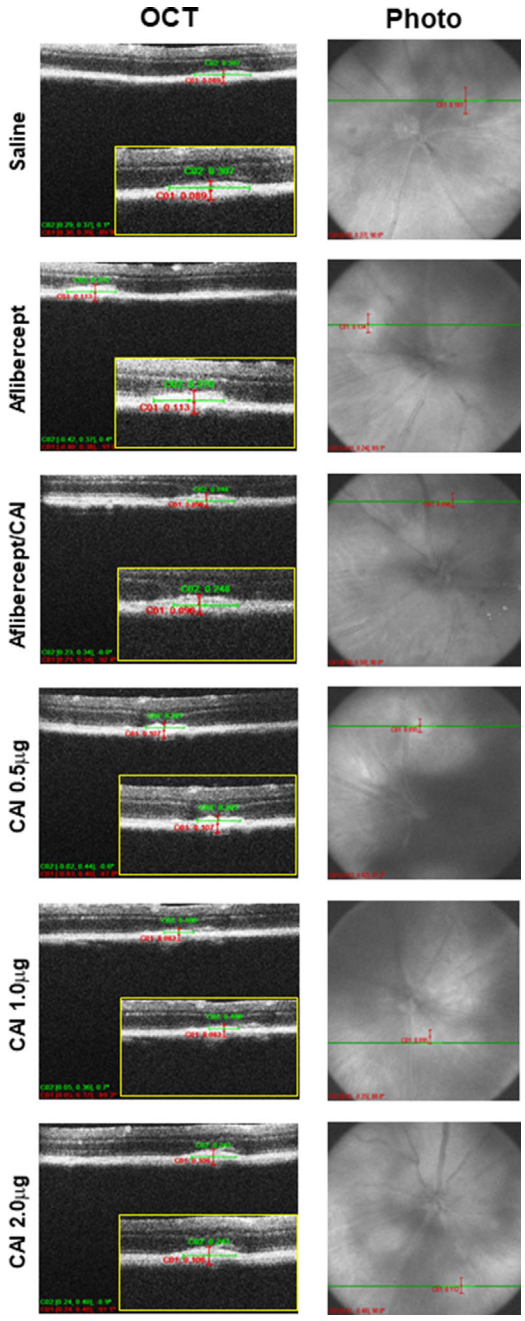

Figure 3. Polymeric CAI-PLGA nanoemulsion reduces CNV lesion size. (**A**) Representative horizontal OCT images with identification of lesion height (*red*) and length (*green*) (*left panel*) and enface image showing perpendicular view with depth of lesion (*red*). Images of saline and CAI-nanoparticle treated mouse retinas at 2 weeks post-injection.

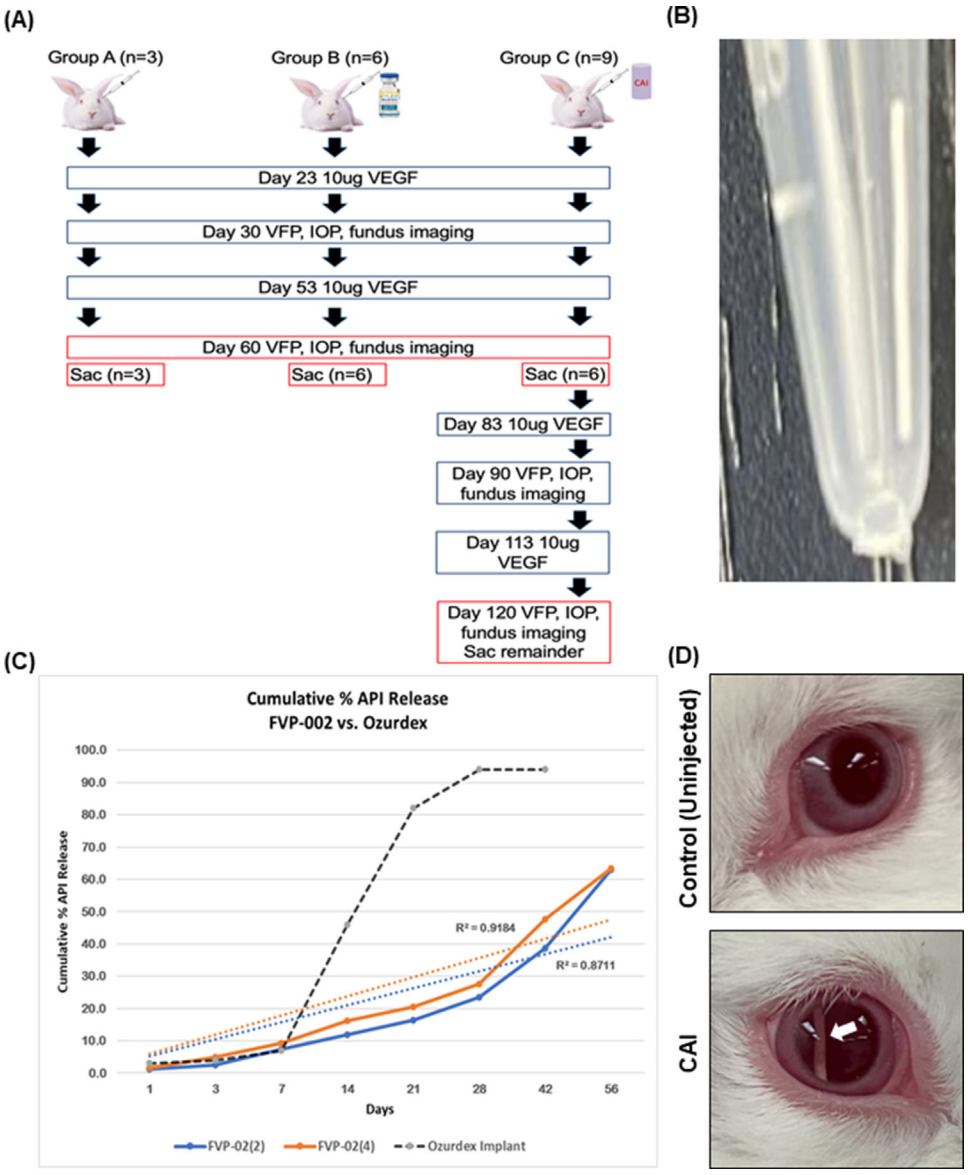

Figure 4. CAI-PLGA implants compared to aflibercept in rabbit model of vascular permeability. (**A**) Study design and time course for rabbit model of proliferative retinopathy. (**B**) Image of CAI PLGA implant. (**C**) Cumulative release of CAI from PLGA implants over time, and (**D**) OD showing implant at postoperative day 1 in the CAI cohort, indicated by the *white arrow*.

CAI-Implant and Inhibition of Rabbit Retinal Permeability

CAI bioresorbable implants (Figs. 4A, 4B) were evaluated in the rabbit model. Initial IVR testing was performed on two formulations to provide information on the release kinetics of CAI in specifically selected PLGA polymers. CAI release was seen to be stable, linear, and predictable over the course of the testing period for both formulations. The determinative bioeffective dose of CAI in serum is 1 to 10 µM, but in the low protein environment of the eye a concentration of 500 nM was found to produce significant anti-angiogenic effects.[14] Figure 4C demonstrates the results of the IVR testing, plotted as cumulative percent drug release over time for both formulations. A comparison to equivalent Ozurdex release data, reproduced from the literature, shows the CAI-implant to have a more linear and consistent active pharmacological ingredient (API) release versus the literature control, which uses a similar class of PLGA delivery system. Visualization of the CAI-implant ex vivo is shown in Figure 4B and in vivo is shown in Figure 4D.

Fundus imaging on day 60 (Fig. 5A) revealed significantly more vascular hyperemia in the saline group compared with the aflibercept and the CAI-

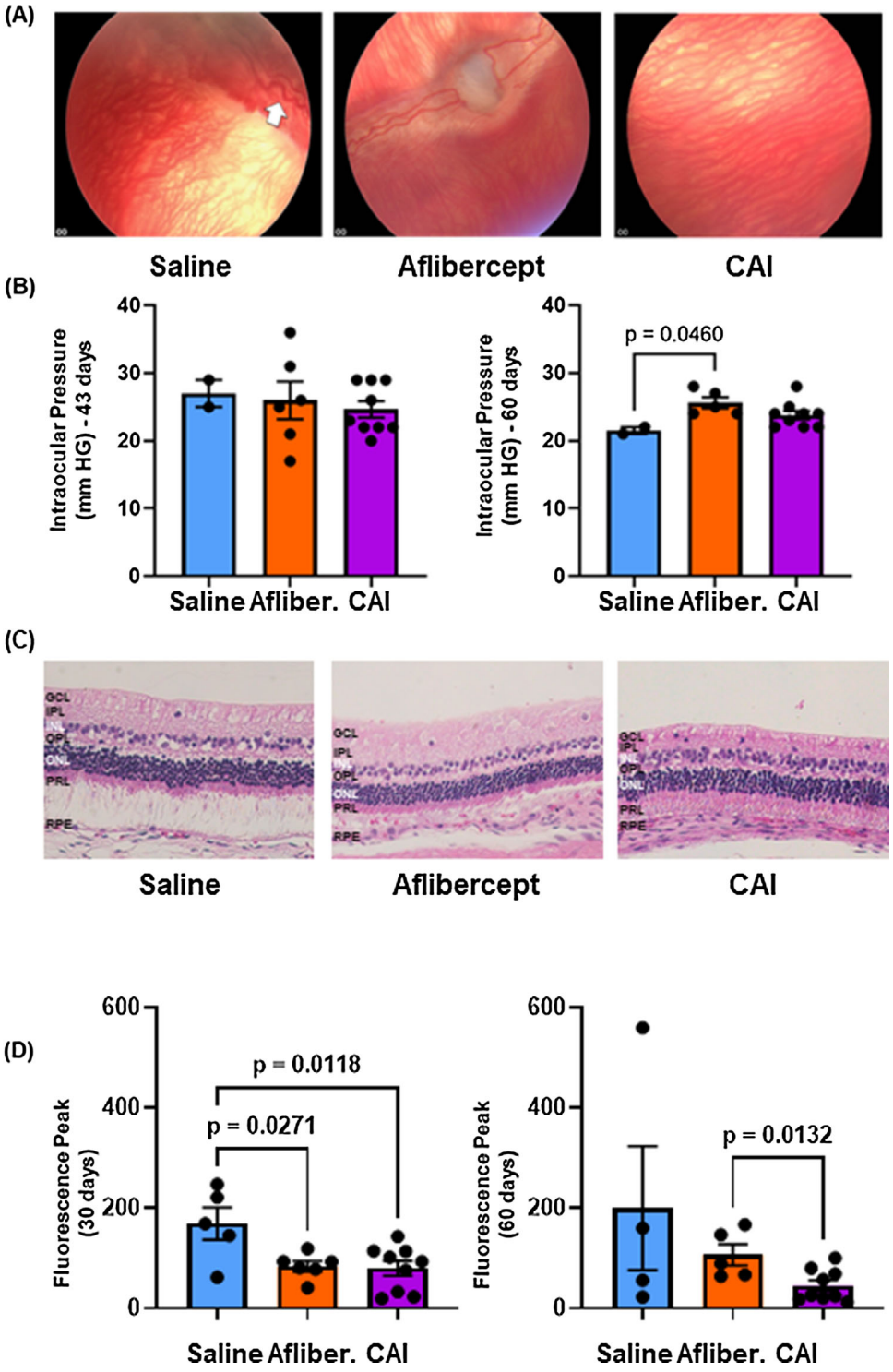

Figure 5. **CAI-PLGA implants inhibit proliferative retinopathy phenotype compared with aflibercept in rabbits.** (**A**) Representative fundus images from saline, aflibercept treated, and CAI treated groups on day 60. Note the tortuosity of vessels (*white arrow*) and overall hyperemia seen in the saline group that is absent in the aflibercept and CAI groups. (**B**) Average intraocular pressure measurements in all 3 cohorts after 30 and 60 days. (**C**) Representative histologic image of retina and retinal cell layers from the sham, aflibercept, and CAI groups. (**D**) Vitreous fluorophotometry results of saline, aflibercept, and CAI treated rabbits.

implant treated groups. In addition, qualitatively, significantly less vascular hyperemia was observed with the CAI-implant treated animals than aflibercept treated animals. Intraocular pressure measurements (Fig. 5B) showed no difference on day 43 but showed an increase with aflibercept on day 60. Retinal thickness measurements were comparable between the treatment groups and no inflammation was noted post-injection or at any later timepoints in the CAI-implant group (Fig. 5C).

Vitreous fluorophotometry revealed significantly lower levels of fluorescein in the aflibercept and CAI-implant groups compared to saline on day 30 (saline = 178.12 ng/mL ± 30.55, $n = 5$ versus aflibercept = 84.40 ng/mL ± 10.45, $n = 6$, $P = 0.0244$, saline versus CAI = 80.16 ng/mL ± 15.02, $n = 9$, $P = 0.0141$). On day 30, the reduction of peak vitreous fluorescence was similar between aflibercept and CAI-implant. On day 60 (saline = 200.03 ng/mL ± 123.64, $n = 4$ versus aflibercept = 107.06 ng/mL ± 18.09, $n = 5$, $P = 0.431$, saline versus CAI = 45.572 ng/mL ± 10.39, $n = 9$, $P = 0.078$; Fig. 5D). On day 60, while the aflibercept treatment effect began to diminish, the CAI-implant treatment effect continued to improve in terms of reduction of vascular permeability. The CAI-implant treated animals demonstrated a two-fold reduction in permeability as measured by fluorescence as compared to aflibercept (aflibercept = 107.06 ng/mL ± 18.09 versus CAI = 45.572 ng/mL ± 10.39, $n = 9$, $P = 0.0132$). The improvement in vascular hyperemia of CAI compared to aflibercept was supported by fundus examination (see Fig. 5D).

Discussion

The salient findings of this study include that the polymeric CAI-PLGA nano emulsion reduced CNV lesion size in the AMD model induced by laser injury. The addition of aflibercept to CAI nanoparticles did not provide further anti-angiogenic efficacy as compared with CAI nanoparticles alone. In vitro release rates of CAI from PLGA bioresorbable implants demonstrate feasibility for 6-month sustained release of bioactive doses following a single intravitreal administration. The intravitreal injection of CAI-PLGA bioresorbable implants in a rabbit model of retinal leakage demonstrated that the implant effectively reduces vascular leakage with no evidence of toxicity, and that corresponds to the time course of release of bioactive concentrations from the CAI-implant in vitro. In addition, both formulations were found to be safe based on multiple measurements which agree with the extensive safety profile of CAI as a systemic agent in human disease. CAI is a pleiotropic angiogenic inhibitor which differentiates this compound from all the standard of care treatments for neovascular retinal disease currently in use and that are in the pipeline. Taken together, these data demonstrate that the CAI-PLGA formulations have many positive attributes that should be applied to human neovascular ocular diseases.

The multiple actions of CAI have garnered its attention as a potential oral therapy for various malignancies, with numerous clinical trials investigating its effectiveness. CAI was administered to over 900 patients with advanced cancer.[16,17,23] CAI is over 99% bound to plasma protein, which combined with variable oral bioavailability, narrowed the therapeutic window of systemic administration. We tested whether local delivery of CAI to the eye would be tolerated compared to the higher concentration burden resulting from systemic exposure, and that the efficacy of CAI will be enhanced in the low protein environment of the eye. Thus, we chose to complex CAI to PLGA for local ocular administration to maximize efficacy, increase durability, and minimize any systemic effects.

The anti-angiogenic activity of CAI is due to its activity against the Orai1 protein, a key subunit in $Ca2^{+}$- release activated $Ca2^{+}$ channel (CRAC). The CRAC channel is important in VEGF-evoked $Ca2^{+}$ entry in endothelial cells (Fig. 6).[11] Increases in intracellular calcium concentrations stimulate endothelial cell proliferation, adhesion, and migration. Additionally, CAI inhibits other key mediators of angiogenesis, including VEGF, HIF-1α, Wnt, MMP-2, c-fos, and viral-like 30 elements (VL30).[24–27]

The Wnt5a-Norrin pathway was recently identified as an important mediator of human neovascular ocular disease where monthly intravitreal injections of a trivalent antibody agonist produced potent anti-neovascular and anti-permeability effects in phase I clinical trials. Once Wnt5a binds to its receptor, protein kinase C is activated which then phosphorylates and deactivates the Orai1 channel. Because CAI binding also inactivates the Orai1 channel blocker, Wnt5a signaling and CAI action are intricately linked (see Fig. 6).

We also tested a combination approach by adding CAI to aflibercept. As Orai1 co-localizes with VEGFR2, CAI likely can possess inherent anti-VEGF activity through this receptor cross talk. However, we did not observe any additional anti-angiogenic effect by combining the two compounds. This is consistent with data from the Restoret (AMARONE) trial (NCT05919693) where combining Restoret with

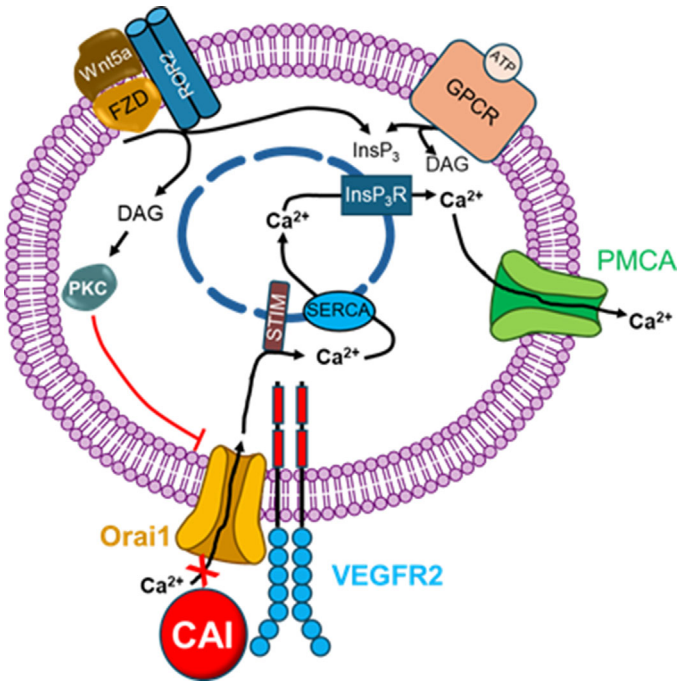

Figure 6. CAI mechanism of action. CAI blocks VEGF action by modulation of the Orai1 channel which is responsible for mediating intracellular calcium concentration. Disruption of Orai1 decreases key angiogenic processes such as tube formation and endothelial cell migration. Orai1 and the VEGFR2 receptor co-localize, and CAI blocks the action of VEGF2 when bound to Orai1. CAI also inhibits pathological angiogenesis via Wnt-Norrin pathways. Modified from Sci China Life Sci. doi: 10.1007/s11427-016-5087-5.

aflibercept did not have additional benefit for patients with neovascular AMD. Use of these two drugs involves interaction between the VEGF and Wnt pathways, which have overlap in their downstream signaling components resulting in no additional benefit or inhibition of the VEGF pathway alone. In our case, the Wnt pathway is linked to Orai1 action which is also inherently involved with VEGF action and thus it is not surprising that we did not see any benefit of the combination over each drug alone (see Fig. 6).

Previously, CAI was found to reduce the size of granuloma formation, reduce serum levels of IL-1β and TNF-α, reduce edema, and reduce paw edema.[28] The anti-inflammatory effects of CAI may contribute to its anti-fibrotic effects. In a study by Guo et al., CAI administration was found to reduce collagen deposition in the colons of murine models of inflammatory bowel disease and significantly decrease levels of TGF-β1 which was dose dependent.[29] Based on these data, CAI may limit progressive fibrosis which otherwise occurs with the current available treatments for neovascular AMD.

The effects of CAI on calcium influx led to increases in Bcl-2 protein. Thus, CAI can exert a neuroprotective effect through prevention of optic nerve damage. Administration of CAI has been shown to increase levels of Bcl-2 and decrease TUNEL-positivity in retinal cells in mice models of retinal neovascularization.[30] CAI may also have effects on cellular aging and senescence, as has been shown to increase expression of SIRT1 in mice models of cancer-related cachexia. This effect may be attributable to the anti-inflammatory properties of CAI that downregulate NF- κB signaling, FoxO3, and ubiquitin and E3 ligase expressions.[31] In addition, CAI modulates the activity of the NLRP3 inflammasome which is a target of atrophic AMD therapy. Thus, CAI may be able to also address the progressive atrophy that limits vision during current treatments of neovascular AMD.

Conclusions

An unmet clinical need exists for additional agents to treat retinal permeability that results from AMD and DR in individuals that are refractory to current treatment options. In this study, we provide a possible addition to the current pharmacological armamentarium by successful generation of CAI formulations for intraocular delivery which were well tolerated and efficacious. In the laser-induced CNV model, CAI-polymeric CAI-PLGA nanoemulsion resulted in robust inhibition of angiogenesis and the combination of aflibercept, and CAI nanoparticles did not provide further anti-angiogenic efficacy as compared to CAI nanoparticles alone. We show the bioresorbable CAI implant worked well as a potent monotherapy in terms of vascular permeability in the rabbit model, which simulates DME pathophysiology. We successfully achieved two critical unmet needs in the current treatment paradigm for neovascular retinal disease by identification of a compound that does not rely solely on blocking the VEGF pathway and second, both the CAI-nano and the CAI-implant represent key steps in the development of more durable administration schemas.

Acknowledgments

Supported by NEI: grants R01 EY033620, EY032753, EY012601, EY035539, EY025383.

Disclosure: **S. Li Calzi**, None; **A. Fujihashi**, None; **D. Chakraborty**, None; **Y. Adu-Rutledge**, None; **R. Prasad**, None; **E.L.V. Ready**, None; **S. Paul**, None;

S. Kakumanu, None; **X. Qi**, None; **M.E. Boulton**, None; **A.J. Franklin**, Founder and Chairman of ForwardVue Pharma (O); **B.H. Katz**, CEO of ForwardVue Pharma (O); **M.B. Grant**, None

[*] SLC and AF contributed equally to this work.

References

1. *Age-Related Macular Degeneration (AMD) Tables*. National Eye Institute. Accessed June 11, 2023. 2023. Available at: https://www.nei.nih.gov/sites/default/files/health-pdfs/WYSK_AMD_English_Sept2015_PRINT.pdf.
2. *Diabetic Retinopathy Tables*. National Eye Institute. Accessed June 11, 2023. 2023. Available at: https://www.nei.nih.gov/learn-about-eye-health/eye-health-data-and-statistics/diabetic-retinopathy-data-and-statistics/diabetic-retinopathy-tables#:~:text=View%20tables%20showing%20prevalence%20rates%20of,diabetic%20retinopathy%20in%20the%20United%20States.
3. Rein DB, Zhang P, Wirth KE, et al. The economic burden of major adult visual disorders in the United States. *Arch Ophthalmol*. 2006;124:1754–1760.
4. Mazzitelli JA, Smyth LCD, Cross KA, et al. Cerebrospinal fluid regulates skull bone marrow niches via direct access through dural channels. *Nat Neurosci*. 2022;25:555–560.
5. Willis JR, Doan QV, Gleeson M, et al. Vision-related functional burden of diabetic retinopathy across severity levels in the United States. *JAMA Ophthalmol*. 2017;135:926–932.
6. Mazhar K, Varma R, Choudhury F, et al. Severity of diabetic retinopathy and health-related quality of life: the Los Angeles Latino Eye Study. *Ophthalmology*. 2011;118:649–655.
7. Yang S, Zhao J, Sun X. Resistance to anti-VEGF therapy in neovascular age-related macular degeneration: a comprehensive review. *Drug Des Devel Ther*. 2016;10:1857–1867.
8. Rofagha S, Bhisitkul RB, Boyer DS, Sadda SR, Zhang K, SEVEN-UP Study Group. Seven-year outcomes in ranibizumab-treated patients in ANCHOR, MARINA, and HORIZON: a multicenter cohort study (SEVEN-UP). *Ophthalmology*. 2013;120:2292–2299.
9. Nicolo M, Ferro Desideri L, Vagge A, Traverso CE. Faricimab: an investigational agent targeting the Tie-2/angiopoietin pathway and VEGF-A for the treatment of retinal diseases. *Expert Opin Investig Drugs*. 2021;30:193–200.
10. Wykoff CC, Singer MA. AMARONE Shows Promising Outcomes for a Novel Treatment Pathway in DME and nAMD -Activation of the Wnt pathway shows a dramatic effect. *Retinal Physician*. 2024;21, https://www.retinalphysician.com/issues/2024/april/amarone-shows-promising-outcomes-for-a-novel-treatment-pathway-in-dme-and-namd/.
11. Li J, Cubbon RM, Wilson LA, et al. Orai1 and CRAC channel dependence of VEGF-activated Ca2+ entry and endothelial tube formation. *Circ Res*. 2011;108:1190–1198.
12. Gross S, Hooper R, Tomar D, et al. Suppression of Ca(2+) signaling enhances melanoma progression. *EMBO J*. 2022;41:e110046.
13. Perabo FG, Wirger A, Kamp S, et al. Carboxyamido-triazole (CAI), a signal transduction inhibitor induces growth inhibition and apoptosis in bladder cancer cells by modulation of Bcl-2. *Anticancer Res*. 2004;24:2869–2877.
14. Afzal A, Caballero S, Palii SS, et al. Targeting retinal and choroid neovascularization using the small molecule inhibitor carboxyamidotriazole. *Brain Res Bull*. 2010;81:320–326.
15. Cruysberg LPJ, Franklin AJ, Sanders J, et al. Effective transscleral delivery of two retinal anti-angiogenic molecules: carboxyamido-triazole (CAI) and 2-methoxyestradiol (2ME2). *Retina*. 2005;25:1022–1031.
16. Si X, Wang J, Cheng Y, et al. A phase III, randomized, double-blind, controlled trial of carboxyamidotriazole plus chemotherapy for the treatment of advanced non-small cell lung cancer. *Ther Adv Med Oncol*. 2020;12:1758835920965849.
17. Hussain MM, Kotz H, Minasian L, et al. Phase II trial of carboxyamidotriazole in patients with relapsed epithelial ovarian cancer. *J Clin Oncol*. 2003;21:4356–4363.
18. Dutcher JP, Leon L, Manola J, et al. Phase II study of carboxyamidotriazole in patients with advanced renal cell carcinoma refractory to immunotherapy: E4896, an Eastern Cooperative Oncology Group Study. *Cancer*. 2005;104:2392–2399.
19. Sulaiman RS, Quigley J, Qi X, et al. A simple optical coherence tomography quantification method for choroidal neovascularization. *J Ocul Pharmacol Ther*. 2015;31:447–454.
20. Silva RLE, Kanan Y, Mirando AC, et al. Tyrosine kinase blocking collagen IV-derived peptide suppresses ocular neovascularization and vascular leakage. *Sci Transl Med*. 2017;9:eaai8030.
21. Iwase T, Oveson BC, Hashida N, et al. Topical pazopanib blocks VEGF-induced vascular leakage and neovascularization in the mouse retina but is

ineffective in the rabbit. *Invest Ophthalmol Vis Sci*. 2013;54:503–511.
22. Dickmann LJ, Yip V, Li C, et al. Evaluation of fluorophotometry to assess the vitreal pharmacokinetics of protein therapeutics. *Invest Ophthalmol Vis Sci*. 2015;56:6991–6999.
23. Omuro A, Beal K, McNeill K, et al. Multicenter phase IB trial of carboxyamidotriazole orotate and temozolomide for recurrent and newly diagnosed glioblastoma and other anaplastic gliomas. *J Clin Oncol*. 2018;36:1702–1709.
24. Bauer KS, Cude KJ, Dixon SC, Kruger EA, Figg WD. Carboxyamido-triazole inhibits angiogenesis by blocking the calcium-mediated nitric-oxide synthase-vascular endothelial growth factor pathway. *J Pharmacol Exp Ther*. 2000;292:31–37.
25. Figg WD, Cole KA, Reed E, et al. Pharmacokinetics of orally administered carboxyamido-triazole, an inhibitor of calcium-mediated signal transduction. *Clin Cancer Res*. 1995;1:797–803.
26. Kohn EC, Alessandro R, Spoonster J, Wersto RP, Liotta LA. Angiogenesis: role of calcium-mediated signal transduction. *Proc Natl Acad Sci USA*. 1995;92:1307–1311.
27. Oliver VK, Patton AM, Desai S, Lorang D, Libutti SK, Kohn EC. Regulation of the pro-angiogenic microenvironment by carboxyamidotriazole. *J Cell Physiol*. 2003;197:139–148.
28. Guo L, Ye C, Chen W, et al. Anti-inflammatory and analgesic potency of carboxyamidotriazole, a tumorostatic agent. *J Pharmacol Exp Ther*. 2008;325:10–16.
29. Guo L, Ye C, Hao X, et al. Carboxyamidotriazole ameliorates experimental colitis by inhibition of cytokine production, nuclear factor-kappaB activation, and colonic fibrosis. *J Pharmacol Exp Ther*. 2012;342:356–365.
30. Franklin AJ, Jetton TL, Kuchemann CL, Russell SR, Kohn EC. CAI is a potent inhibitor of neovascularization and imparts neuroprotection in a mouse model of ischemic retinopathy. *Invest Ophthalmol Vis Sci*. 2004;45:3756–3766.
31. Chen C, Ju R, Zhu L, et al. Carboxyamidotriazole alleviates muscle atrophy in tumor-bearing mice by inhibiting NF-kappaB and activating SIRT1. *Naunyn Schmiedebergs Arch Pharmacol*. 2017;390:423–433.